RMetS

Royal Meteorological Society

A preliminary study to investigate the biogeophysical impact of desertification on climate based on different latitudinal bands

Ye Wang,[a]* Xiaodong Yan[b] and Zhaomin Wang[c]

[a] *College of Civil Aviation, Nanjing University of Aeronautics and Astronautics, People's Republic of China*
[b] *State Key Laboratory of Earth Surface Processes and Resource Ecology (ESPRE), College of Global Change and Earth System Science, Beijing Normal University, People's Republic of China*
[c] *British Antarctic Survey, Cambridge, UK*

ABSTRACT: Desertification is an international environmental challenge which poses a risk to portions of over 100 countries. Research into desertification and climate change has the potential to contribute to natural resources management and adaptation to climatic and other changes in Earth systems. An Earth system model of intermediate complexity (EMIC), the McGill Paleoclimate Model-2 (MPM-2) was used to explore the climatic biogeophysical effects of desertification in different latitude bands from 1700 to 2000 AD. It was found that latitudinal-band desertification attributable to forest and grass removal caused global cooling, land surface albedo increasing and precipitation reduction in the Northern Hemisphere as well as heat transport increasing in global ocean. These results highlighted global climate reaction to local desertification and demonstrated that the location of the desertification projected a potentially differential impact on local and global climate. That was, desertification in 0°–15°N gave a somewhat minor effect on global and local climate; desertification in 45°–60°N caused a significant reduction in global temperature while desertification in 15°–30°N induced a prominent reduction in local temperature. In response to desertification, surface albedo change as a forcing was the dominant biogeophysical driver of climate over the Northern Hemisphere while precipitation change as a response was probably the primary driver of climate over the Southern Hemisphere. Overall, the regional desertification may cause a global climatic effect, especially concerning desert expansion along the 15°–30°N and 45°–60°N latitude bands, which led to a more prominent effect on the Earth's climate and even oceanic circulation. The results of this study provide useful information when comparing the effects of desertification in different latitude bands on climate.

KEY WORDS   desertification; climate change; modelling

Received 22 January 2013; Revised 4 May 2015; Accepted 5 May 2015

1. Introduction

As a world-wide phenomenon, desertification affects about two-thirds of the countries of the world, and one-third of the earth's surface, on which millions of people live (Reynolds and Stafford Smith, 2002; United Nations Sudano-Sahelian Office, 2002). It also causes the earth's ecosystems to deteriorate. Definitions of desertification are usually broad; in this article it is presented as the loss of vegetation or replacement of forest or/and grassland with desert (Hill *et al.*, 1995; Ash *et al.*, 2002). This desertification affects global climate via biogeochemical and biogeophysical processes.

Biogeophysical consequences of desertification include its effects on changes in albedo, transpiration and surface roughness. In general, replacing forest and grassland with desert leads to an increase in land surface albedo and a decrease in transpiration. Such expansion of desert decreases surface roughness affecting the energy and momentum balances in the boundary layer by decreasing the ability of air to mix. Desertification and its influence on climate change have become the research focus of many scholars in the past few decades (Li *et al.*, 2000). Proposing a biogeophysical feedback mechanism linking vegetation, albedo and precipitation as a partial explanation for recurrent drought in desert border areas, Charney *et al.* (1975) show that the radiative heat loss caused by the high albedo of a desert contributes significantly to the sinking and drying of the air aloft and therefore to the reduction of precipitation. Zheng and Eltahir (1997) suggest that the potential impact of desertification on regional climate depends critically on its location. That is, desertification near the southern edge of the Sahara reduces the rainfall within the perturbation region but enhances rainfall south of it. Furthermore, desertification appears to be linked to a shift in seasonal precipitation use by vegetation from mainly summer to winter inputs, resulting in an apparent decoupling of vegetation responses to inter-annual monsoonal variation (Asner and Heidebrecht, 2005). Souza and Oyama (2011) find that a pronounced and significant

* Correspondence to: Y. Wang, College of Civil Aviation, Nanjing University of Aeronautics and Astronautics, 29 Yudao Street, Nanjing 210016, People's Republic of China. E-mail: wytea@126.com

precipitation reduction in large parts of semi-arid area of Northeast Brazil (SANEB) is resulted from total desertification. In addition, Alkama *et al.* (2012) show that the main impact of replacing the vegetation by bare soil on the energy budget is a large reduction in upward latent heat transfer and a warming over tropical forests and a slight cooling over semi-arid and arid areas in south of 20°N. However, most of these studies focus on desertification on a small scale. Relative little attention has been given to the impact of desertification in different latitude bands on the regional and global climate because of its different climate background of the atmospheric and (wind driven) ocean circulation caused by the differential solar heating over latitudinal bands.

Furthermore, various studies have simulated vegetation loss effects from the standpoint of land cover changes. Historical forest removal at mid-latitudes has increased land surface albedo which has cooled the Northern Hemisphere (NH) climate (Bonan, 1997; Brovkin *et al.*, 1999; Betts, 2001; Govindasamy *et al.*, 2001; Bounoua *et al.*, 2002; Brovkin *et al.*, 2006; Pitman *et al.*, 2009; Lee *et al.*, 2011). On the other hand, although the climate response to tropical deforestation is more equivocal, some previous studies suggest that large-scale removal of tropical forests could reduce evapotranspiration rates, leading to decreased latent heat fluxes. This causes a higher Bowen ratio and thus an increase in land surface temperature (Henderson-Sellers *et al.*, 1993; Lean and Rowntree, 1997; De Fries *et al.*, 2002; Feddema *et al.*, 2005; Brovkin *et al.*, 2009). So it has been suggested that the effects of forest removal are different in the tropics and at mid-high latitudes (Claussen *et al.*, 2001; Pielke *et al.*, 2002; Bala *et al.*, 2007; Betts *et al.*, 2007; Bonan, 2008). However, the relative importance of vegetation loss in different latitudes has never been quantified (Davin and Noblet-Ducoudré, 2010).

In addition, most of the previous desertification and vegetation loss experiments have been performed using Atmospheric General Circulation Models (AGCMs) without interactive ocean models, while the climate changes induced by land surface changes are affected by feedbacks from sea surface temperature (SST) and sea ice, including the thermohaline circulation of the ocean. There are also suggestions that desertification may be associated with climate change in other parts of the world, particularly through changes in ocean temperatures (Warren and Khogali, 1992; Williams and Balling, 1994). Besides, it is the ocean that triggers climate variability in the Sahel at interannual to interdecadal time scales (Giannini and Biasutti, 2008), while the response of annual mean meridional oceanic heat transport to desertification has never been assessed, thus preventing a more comprehensive understanding of the overall biogeophysical effects of desertification. In light of the little study on desertification over areas except Sahel and the rarely quantified desertification effects over different latitudes as well as the importance of interactive ocean on desertification effects, we use an EMIC, MPM-2 (Wang and Eltahir, 2000), to address the impact of desertification over different latitudes in a more comprehensive manner in this study. Therefore, the main goal of this study is to assess the biogeophysical effects of forest and grass replacement with desert over different latitudes on shaping the global and regional climate.

Vegetation loss or forest or/and grass replacement with desert also alters direct emissions of CO_2 into the atmosphere which modifies the Earth's energy budget and thus climate. Such biogeochemical effect associated with desertification is so significant that it may reverse the overall climate change patterns; while because of the exclusion of carbon cycle model within our climate system model, we focus here on the biogeophysical effects of the desertification on climate. To allow long model integrations and simulate the response with interactive components in Earth system, we use an EMIC, MPM-2 (Wang and Mysak, 2000), to study biogeophysical effects of desertification on climate and their regional effects. EMICs include all the main components of the earth system. Although it simplifies the courses and details using parameterization moderately, it embodies the feedbacks and interactions among the components in climate system. So EMICs can simulate all the main processes in large time scale efficiently to investigate the influence of uncertainty in climatic forcings and process parameterizations on model results through many sensitivity experiments (Forest *et al.*, 2002).

In this paper, MPM-2 is used to explore the effects of desertification in different latitudes, and to estimate the temperature, land surface albedo and precipitation response to the desertification zonally. The response of mean meridional oceanic heat transport to desert expansion is also investigated. Our objective here is neither to reconstruct the observed pattern of desertification, nor to simulate possible scenarios for desertification vividly. Instead, we aim at assessing the magnitude of changes in temperature, land surface albedo and precipitation that is possible in the climate system because of desert expansion based on different latitudinal bands provided whole latitude bands are instantaneously desertified. This contributes to understand how the processes involved in the climate response to desertification might differ between different latitudes.

2. Experimental design

We use the MPM-2, an EMIC, to investigate the biogeophysical effects of desertification. This model has successfully simulated changes in the thermohaline circulation state (Wang and Mysak, 2001; Wang *et al.*, 2002) and the last glacial inception (Wang and Mysak, 2002). It also has been used to study the climate changes on 1000-year scale as Holocene (Wang *et al.*, 2005a, 2005b), and the climatic effects of natural forcings (Shi *et al.*, 2007; Yin *et al.*, 2007; Wang and Yan, 2013; Wang *et al.*, 2013). The atmosphere in the MPM-2 is represented by an energy–moisture balance model in which the meridional energy and moisture transports are parameterized by a combination of advection and diffusion processes. In the ocean model, zonally averaged advection–diffusion equations for temperature and salinity are employed
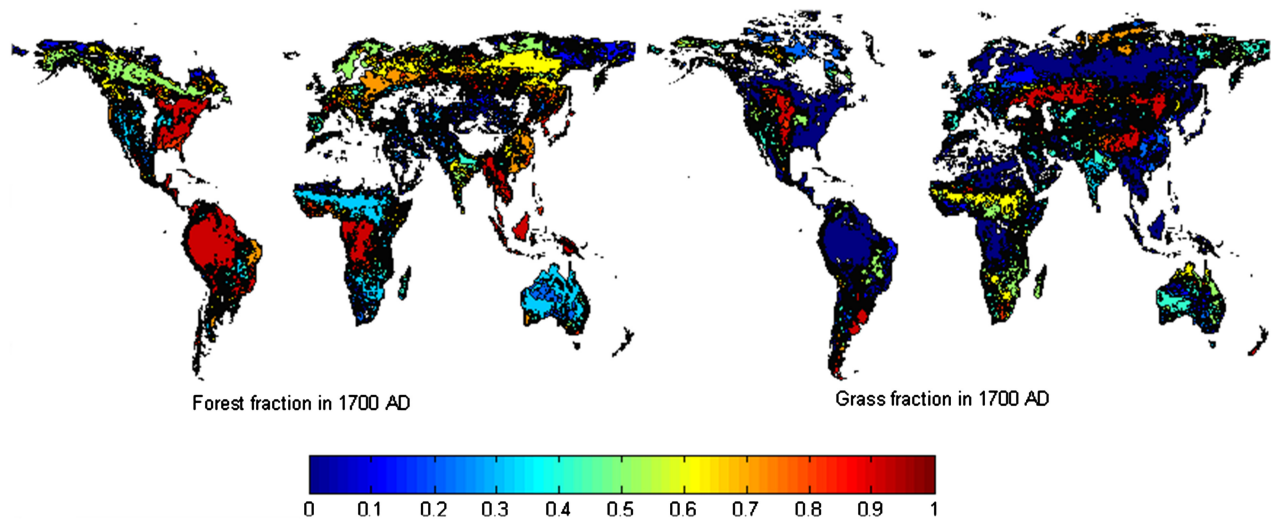
Figure 1. The forest and grass fraction in 1700 AD.

to predict their time evolutions based on vorticity conservation. A zero-layer thermodynamic-dynamic sea-ice model without snow and a land surface model in which the surface temperature predicted using the energy balance equation are used. The ice sheet model in the MPM-2 is the vertically integrated dynamic part of the 2D ice sheet model of Marshall and Clarke (1997). The MPM-2 is also interactively coupled to the dynamical vegetation continuous description model (Brovkin *et al.*, 1997; Wang *et al.*, 2005c). For each grid cell, the tree, grass and desert fractions are predicted as functions of the annual precipitation and the growing degree day index.

In the simulation of desert expansion, the global land cover dataset in 1700 AD are derived from Pongratz *et al.* (2008) at a resolution of 30 min. This dataset specifies 14 land cover classes including three human use types (crop, C3 and C4 pasture) and 11 natural vegetation types in global coverage. For each year, a map that contains 14 fields is provided. Each field holds the fraction the respective vegetation type covers in the total grid cell (0–1). Its 30′ resolution of the dataset is aggregated to the coarse spatial resolution of the model. As for one grid cell, the grass fraction is the sum of crop, grass and pasture; whereas forest fraction is determined by the sum of the remaining types of vegetation, and desert is the percentage of soil that is covered by no vegetation types. The forest and grass fraction in 1700 AD is given in Figure 1. The forest and grass as well as surface land area in different latitude bands are shown in Table 1. A largest vegetation area of 13.89 million km^2 occurs in latitude 45°–60°N and a small vegetation area arises in 0°–15°N.

To investigate the climate in response to land cover variations, two types of numerical experiments are carried out: control and desertification runs. The equilibrium state is reached after a 5300-year integration in order to obtain the same initial conditions. In control experiment (EC), we have chosen to start the runs with 'true world' land cover representations in 1700 AD. In desertification experiment (ED), simulations with global, 0°–15°N,

Table 1. The forest, grass and the surface land area (million km^2) in latitudinal band.

	0°–15°N	15°–30°N	30°–45°N	45°–60°N
Land area	16.73	18.55	26.12	25.60
Forest	7.34	4.98	5.28	8.53
Grass	1.22	5.37	4.46	5.36

15°–30°N, 30°–45°N and 45°–60°N land latitude grids replacement of forest and grass with desert in 1700 AD are performed respectively. The potential impact of latitudinal desertification on regional and global climate is derived by subtracting EC from ED; that is Dall, D0015, D1530, D3045 and D4560, respectively. So Dall, D0015, D1530, D3045 and D4560 denote the subtraction of simulation with 'true world' land cover representation from the simulation with global and latitudinal band replacement of forest and grass with desert in 1700 AD, respectively. These runs are carried out with earth orbital parameters keeping constant at present-day values. Atmospheric CO$_2$ concentration in simulations EC and ED is fixed at a constant level of 280 ppm. In all simulations, atmospheric, oceanic and sea-ice components of EMICs are interactive. Although these extreme designs do not intent to manifest realistic land cover disturbances, they give us a contrast with the global and regional effects of desertification over different latitudes. Desertification can lead to very different impacts depending on whether vegetation is kept at static or dynamic (Wang and Mysak, 2000). After the test of simulations it was found that if the land cover was not static, the simulated dynamic land cover would not be desert and the final results were no longer the effects of desertification. For example, the simulated global temperature was −0.04 °C under static desertification in 0°–15°N, while it was 0.11 °C when the land cover was as an initial condition. So this idealized setting instead of the actual pattern of desertification is a fixed land cover for each simulation.

To assess the regional and seasonal temperature, albedo, precipitation and the mean meridional oceanic heat transport response to desertification, the last 30 years' results of the runs are averaged. Following Pitman *et al.* (2009) and Findell *et al.* (2007) using the modified Student's *t*-test (Zwiers and von Storch, 1995) at the 0.05 level significance, we compare 30-year climatologies at each model grid cell in order to isolate the signal of desert expansion from the model inherent noise. At 95% confidence level, the probabilities that the simulated changes due completely to the variability of the model could be only about 5% (Bounoua *et al.*, 2002). This test is more rigorous than the standard *t*-test because it accounts for autocorrelation within time series, reducing the rate of false positives (Pitman *et al.*, 2009).

3. Results

Desertification alters the surface energy fluxes through a complex interplay of morphological and physiological effects, thus influencing global climate. The overall impact of NH desertification is first investigated to reveal its total biogeophysical effects. In order to assess the relative importance of the desert expansion in different latitudes, the changes in monthly temperature, albedo and precipitation are evaluated on latitude band basis. Analysis for the differences in the surface albedo change which perturbs the radiation budget and precipitation change which affects Bowen ratio will help to understand how the processes involved in the climate response to desertification might differ between different locations. Last, the effects of the NH desertification on mean meridional oceanic heat transport in different latitudes are estimated to obtain a better understanding of the response of earth system to desertification to improve the assessment and monitoring of desertification.

3.1. Overall biogeophysical effects of desertification

As the consequences of latitudinal desertification could extend to the whole planet, the overall biogeophysical effects of the NH desertification are assessed. The impacts of NH desertification on global surface air temperature and sea ice area are summarized in Table 2. The desertification causes a decrease in global, NH and the Southern Hemisphere (SH) temperature with a global average cooling in the range 0.04–1.76 °C based on different desert expansions in this study. The forest and grass removal in 45°–60°N leads to a large decrease in global mean annual temperature which is caused by the largest vegetation removal area (Table 1). The desertification in 0°–15°N has a least overall impact. The cooling in 15°–30°N and 45°–60°N accounts for up to about 43% of the global cooling (1.76 °C) in response to desertification. Owing to the more landmasses and forcing originating in the NH there is a more prominent decrease in the NH temperature in response to replacements of tree and grass with desert. The decrease in temperature because of desertification leads to an increase in sea ice area. Although the replacement

Table 2. The differences in annual mean global, NH, SH surface air temperature and sea ice area of the last year of simulation.

	Dall	D0015	D1530	D3045	D4560
Global-sat[a] (°C)	−1.76	−0.04	−0.37	−0.22	−0.39
Sat-north[b] (°C)	−2.19	−0.05	−0.55	−0.34	−0.59
Sat-south[c] (°C)	−1.33	−0.03	−0.19	−0.11	−0.19
NHamean[d] (10^6 km^2)	0.44	0.01	0.13	0.13	0.29
SHamean[e] (10^6 km^2)	5.17	0.03	0.4	0.17	0.44

[a]Global surface air temperature. [b]Northern Hemisphere surface air temperature. [c]Southern Hemisphere surface air temperature. [d]Northern Hemisphere sea ice area. [e]Southern Hemisphere sea ice area.

of tree and grass with desert leads to a less prominent decrease in the SH temperature, there are more increases in sea ice area in the SH which is because of the larger sea area comparing with that in the NH. Such increases in sea ice area reflect more solar energy and reduce the heat supply from the ocean, which in turn amplifies the decrease of the SH temperature through the sea ice-albedo feedback. Therefore, through these mechanisms, the cooling effects of the reduced solar radiation are amplified by the internal processes in the climate system (Wang and Mysak, 2000).

3.2. Effects of desertification on zonal and monthly temperature, albedo and precipitation

The pronounced local and seasonal effects of desertification on temperature are revealed. The impacts of desertification on temperature are illustrated in Figure 2 and red dotted areas where changes are significant at the 95% confidence level using the modified *t*-test are indicated. Zonally, these averaged changes in seasonal surface air temperature over different latitude bands are statistically significant over 45, 64, 61 and 61% of the grid points as for the simulation of D0015, D1530, D3045 and D4560, respectively. Results from every scenario simulation show a statistically significant impact of latitudinal desertification on the near surface temperature over the regions of desert expansion, which is considerably greater than global effects. However, the magnitude and pattern of local change differs depending on location of desertification. Extensive statistically significant decreases of temperature are mainly in the NH where vegetated surfaces have been changed to desertification. In point of seasonal differences in surface temperature, a maximum cooling of 0.38 °C arises over this latitude during the snow thawing season(spring) (see Figure 2(a)) in response to desert expansion in 0°–15°N, when the vegetation-snow-albedo feedback is most pronounced. This result is in agreement with Bonan *et al.* (1992). The D1530 represents a large vegetation removal area of 10.35 million km^2 over this latitude band, and hence simulated cooling is the most prominent with local temperature decreases typically between 0.4 and 2.5 °C in the NH (Figure 2(b)). This maximum cooling during JJA is in line with Brovkin *et al.* (1999). In D3045 there is a local cooling in the range of 0.2–1.1 °C in the NH which is smaller than that in
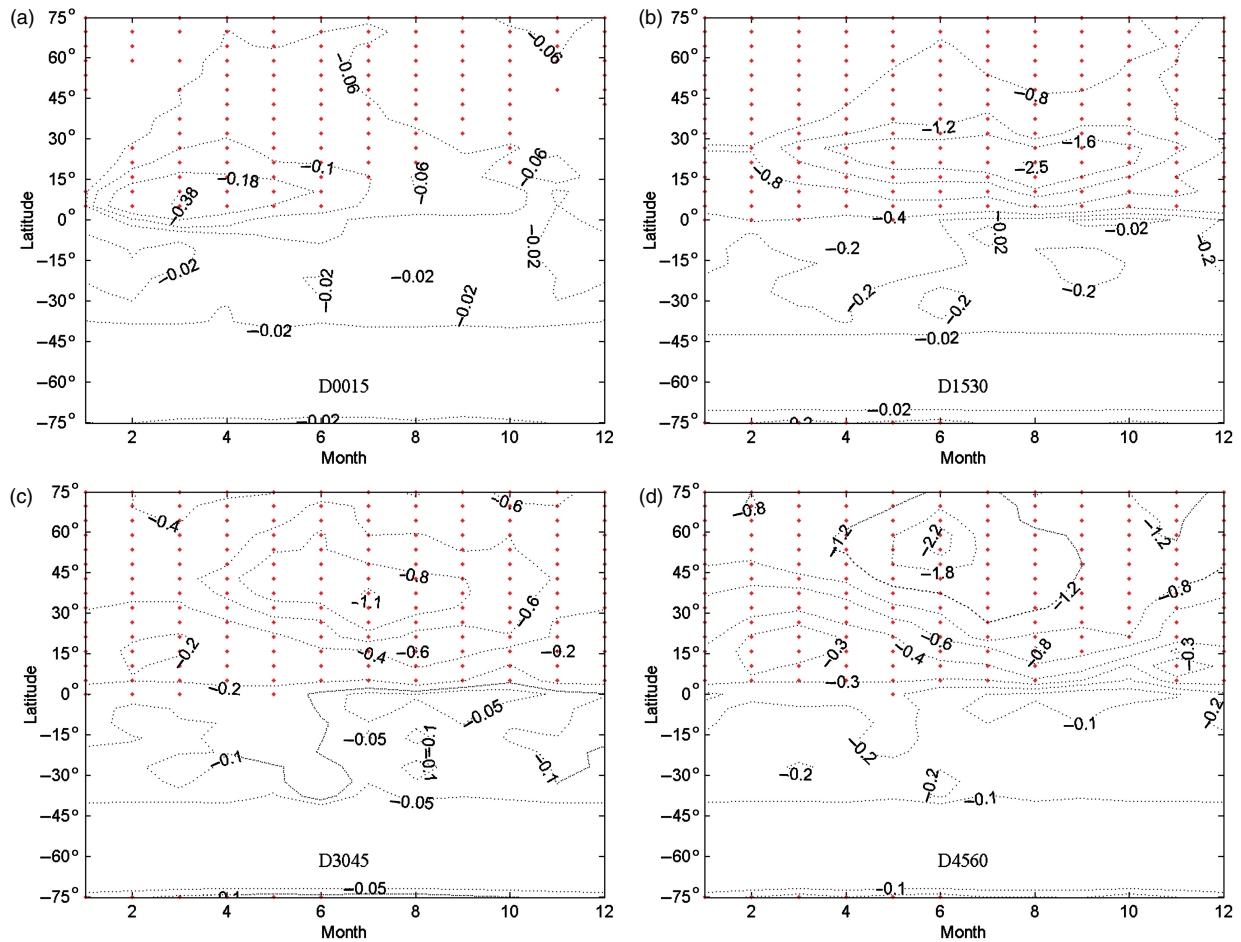
Figure 2. The differences in monthly surface air temperature (°C), the last 30-year averages in desertification simulation from year 1700–2000. (a) D0015; (b) D1530; (c) D3045; (d) D4560. Areas where changes are significant at the 95% confidence level using the modified *t*-test are shown in red dots.

D1530 (Figure 2(c)). This is not surprising given that scenario D3045 projects the low areas of vegetation removal over this latitude band. The forest and grass removal in 45°–60°N leads to a significant cooling of 2.2 °C during JJA (Figure 2(d)). A decrease in temperature to the north of the desertification areas (above 60°N) is not because of direct forcing but rather because of the interaction of the vegetation-snow-albedo effect and sea-ice-albedo effect. Despite the fact that almost none of the temperature differences are significant in a statistical sense, there is a cooling of 0.02–0.2 °C in the SH. The temperature changes in regions distant from the locations where desert expansion has actually changed are accounted for the atmospheric circulation which advects the energy fluxes associated with desertification (Bounoua *et al.*, 2002). The combined action of such atmospheric circulation and the associated changes in SSTs and sea-ice cover propagate the local effects to the global scale.

Any alteration of surface vegetation will have an immediate effect on the albedo of the land surface. The resulting change in surface albedo could have been exerting a radiative forcing of climate which perturbs the radiation budget by modifying the absorption of shortwave radiation. The prominent cooling in response to desertification

is probably accounted for changes in land surface albedo in this study (Figure 3). Conversion from forest and/or grass to desert in this study results in higher land surface albedo. This increased land surface albedo sends more solar radiation back into space (Zeng *et al.*, 1999), and alters the redistribution of solar energy on and near the Earth's surface. Such change in energy budget affects near-surface temperature and precipitation at a local scale. Since this changing global climate resulted from the land vegetation alteration produces modifications in large scale precipitation and temperature patterns which, in turn, modifies the land vegetation. This vegetation modification causes a change in the land surface albedo which thus produces further climatic change. Red dotted areas where land surface albedo changes are significant at the 95% confidence level using the modified *t*-test are shown in Figure 3. Zonally averaged changes in seasonal land surface albedo over different latitude bands are statistically significant over 26, 61, 49 and 55% of the grid points with desertification as for simulation of D0015, D1530, D3045 and D4560, respectively. Statistically significant land surface albedo increase is mainly confined to the forcing originating area in NH. The desert expansion in 0°–15°N leads to a maximum increase of 0.06 in land surface albedo during MAM
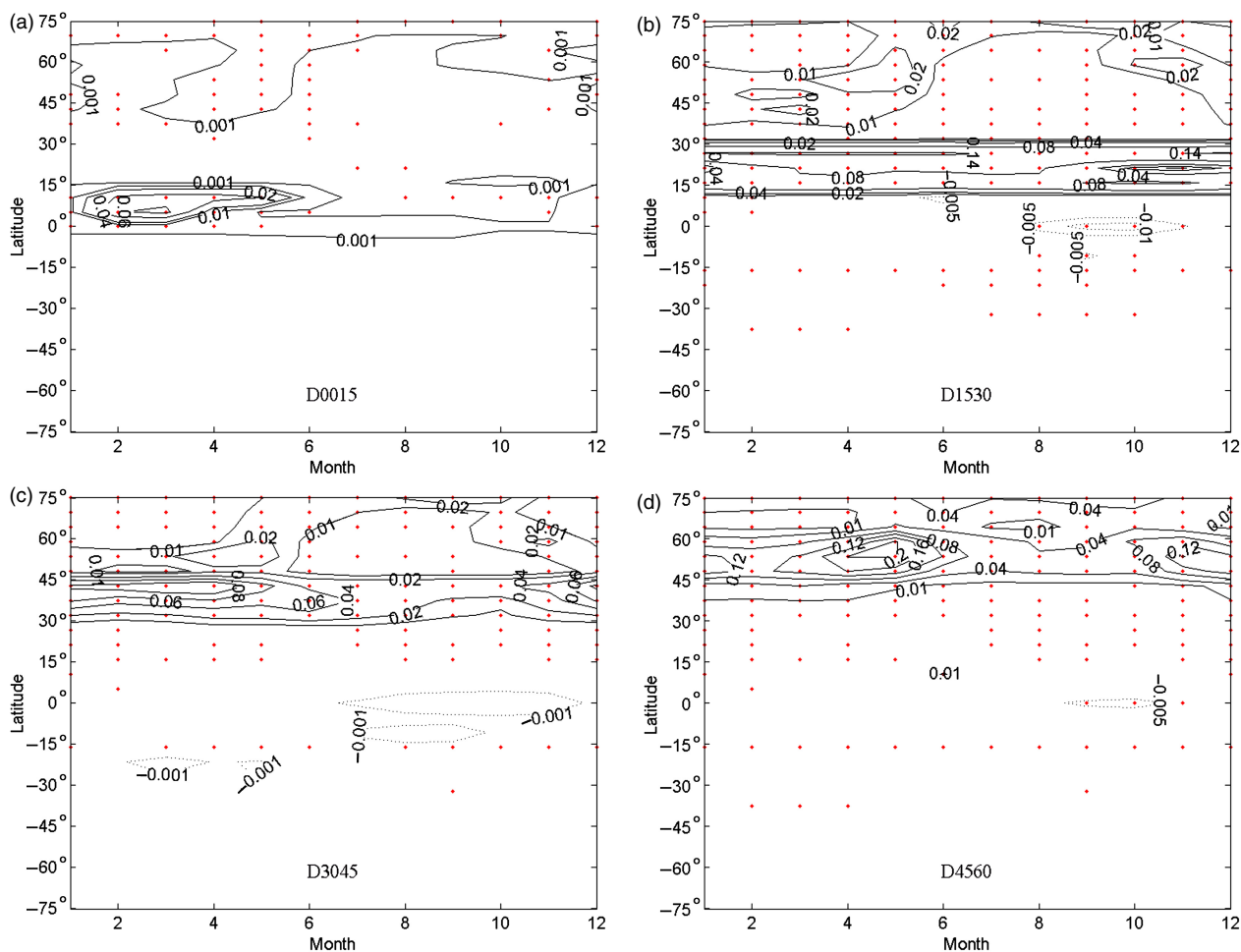
Figure 3. The differences in monthly land surface albedo, the last 30-year averages in desertification simulation from year 1700 to 2000. (a) D0015; (b) D1530; (c) D3045; (d) D4560. Areas where changes are significant at the 95% confidence level using the modified *t*-test are shown in red dots.

(Figure 3(a)), which suggests that this land surface albedo change is the main driver of the significant temperature change (Figure 2(a)) in these regions. The forest and grass removal in 15°–30°N leads to a significant increase of 0.14 in land surface albedo during DJF and MAM (Figure 3(b)). The desert expansion in 30°–45°N leads to an increase of 0.08 in land surface albedo during MAM (Figure 3(c)). The largest increases in land surface albedo of 0.2 are present in the experiment of D4560 during MAM (Figure 3(d)) in response to forest and grass removal.

Precipitation is an important component of the atmosphere which influences climate through the changes of hydrological cycling. There are significant localized and seasonal changes in precipitation in response to desert expansion (Figure 4) and red dotted areas where changes are significant at the 95% confidence level using the modified *t*-test are shown. The differences in seasonal precipitation over different latitude bands are statistically significant over 13, 37, 30 and 36% of the grid points with desertification as for simulation of D0015, D1530, D3045 and D4560, respectively. Statistically significant precipitation decrease is mainly confined to the NH, while the effect of desertification on monthly precipitation differs among scenarios locally. This is the same as the temperature

change in response to desertification. The larger local decrease in temperature is accompanied by a larger local decrease in precipitation in the NH. There is a maximum reduction of 0.18 mm day^{-1} in precipitation over forcing originating area during MAM in D0015 (Figure 4(a)). The desert expansion in 15°–30°N leads to a most pronounced decrease of 0.7 mm day^{-1} during February-March and an increase of 0.4 mm day^{-1} during JJA over forcing originating area in precipitation (Figure 4(b)). There is a maximum decrease of 0.28 mm day^{-1} during February in simulation D3045 (Figure 4(c)). The desert expansion in 45°–60°N leads to a significant decrease with a maximum value of 0.4 mm day^{-1} during February and an increasing of 0.1 mm day^{-1} during JJA over forcing originating area in precipitation (Figure 4(d)). This significant reduced precipitation in February is in line with the IPCC which demonstrates that the largest precipitation changes over northern Eurasia and North America are projected to occur during the winter (IPCC, 2013). In the MPM-2, precipitation is parameterized mainly based on surface air temperature and surface specific humidity. The changes in precipitation are not only caused by the change in temperature and the resulting change in evaporation, but also over the change in sea-ice area that also influences
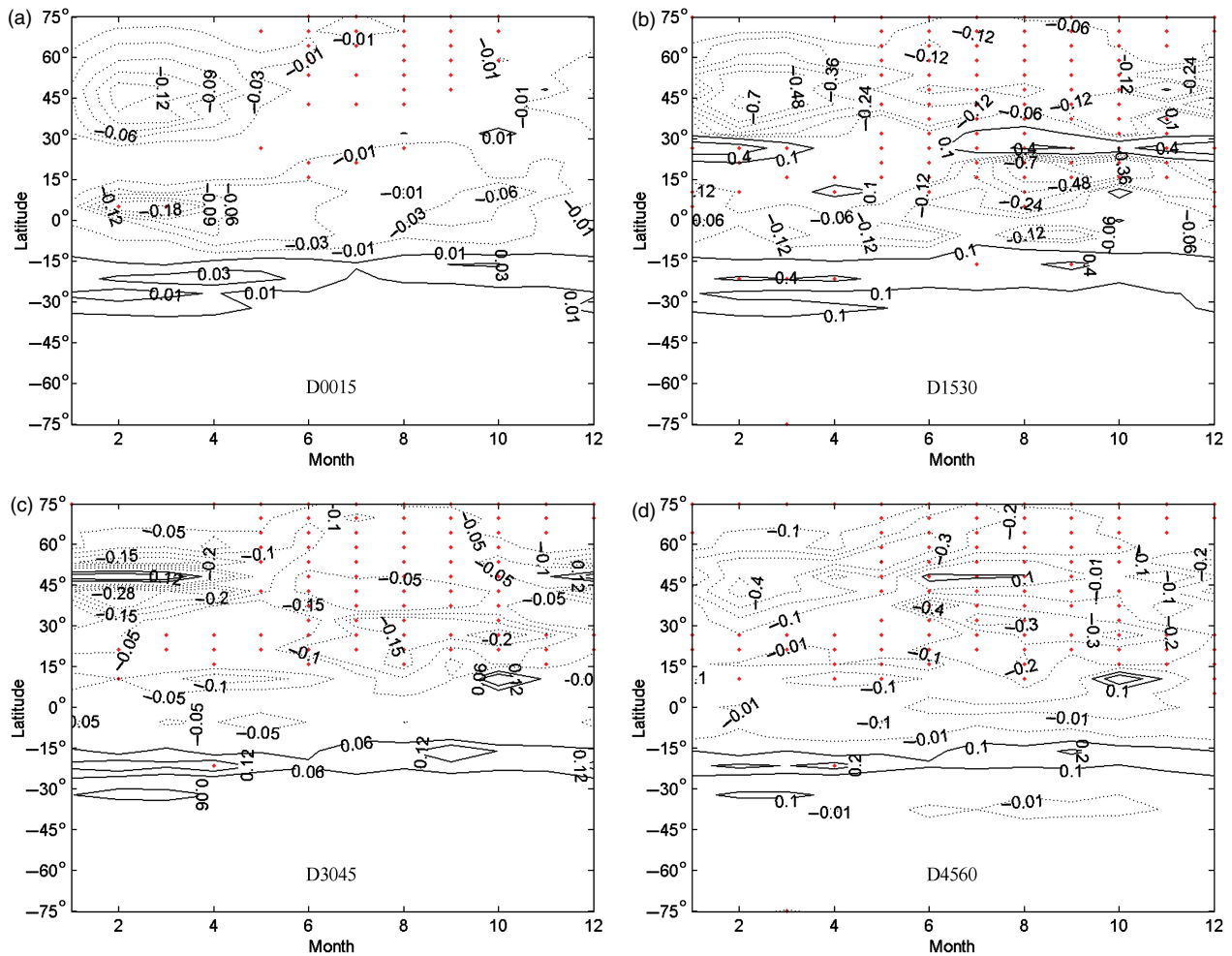
Figure 4. The differences in monthly precipitation (mm day^{-1}), the last 30-year averages in desertification simulation from year 1700 to 2000. (a) D0015; (b) D1530; (c) D3045; (d) D4560. Areas where changes are significant at the 95% confidence level using the modified *t*-test are shown in red dots.

evaporation which controls surface specific humidity. In the most parts of the NH, this decrease in precipitation is because of the reduction of trees and grasses there which are replaced by desert. This weakens the hydrological cycle, leading to less precipitation. The significant reduction in precipitation during February-March is accounted for the obvious sea-ice area in this region during this season, which leads to less evaporation. The increased precipitations in D1530 and D4560 during JJA are probably explained by an increase in the land-ocean temperature gradient. There are increases in precipitation over the SH in response to desert expansion in the NH, although only a small part of the precipitation differences are significant in a statistical sense (Figure 4). The decreases in precipitation over the NH result in a hydrological cycle weakening which causes a reduction of evapotranspiration. This decrease in evapotranspiration is accompanied with a decreased latent heat flux. The reduced disposition of energy from the surface by such latent heat flux results in a warmer surface through increased Bowen ratio (Anderson-Teixeira *et al.*, 2012). So the net change in the NH temperature depends on the warming resulted from the decreases in evapotranspiration and the cooling resulted

from the increases in albedo in response to desertification. While in response to the NH desertification the increased precipitation over low latitudes of the SH leads to increased evaporation. It has a cooling effect on the temperature here via a decreased Bowen ratio, although this precipitation trend is not as statistically significant.

3.3. The response of mean meridional heat transport in global ocean

The climate differences in response to desertification are influenced by reactions from SSTs, sea ice and thermohaline circulation of the ocean. The Atlantic overturning thermohaline circulation (AOTHC) is one of the essential features of the global ocean circulation. The AOTHC is a highly sensitive component of the climate system. In this article, we restrict our attention to the maximum value of the North Atlantic overturning streamfunction (MAOSF). In response to desert expansion in latitudinal bands there is an increase in MAOSF with a maximum value of 1.56 Sv (1 Sv = 10^6 m^3 s^{-1}) in D4560 and a minimum value of 0.05 Sv in D0015. This AOTHC strengthening is accounted for the surface cooling, as it
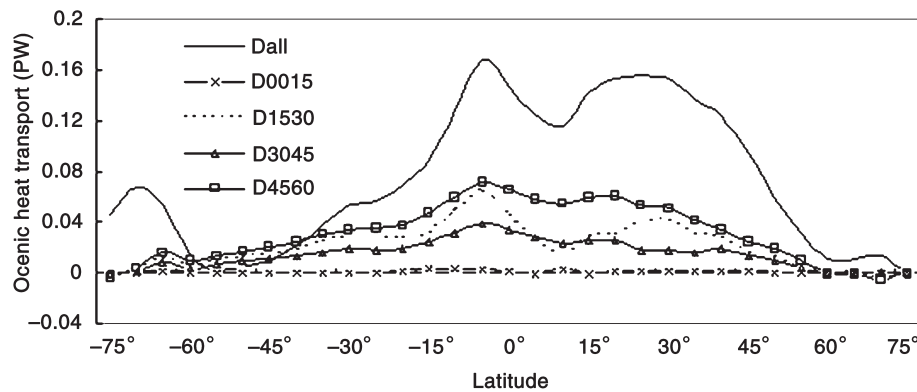
Figure 5. The differences in annual averaged meridional oceanic heat transport, the last 30-year averages in desertification simulation from year 1700 to 2000. 1 PW (petawatts) $= 10^{15}$ W.

increases the density of the surface waters in the North Atlantic, thus promoting deep mixing.

As an important indicator of the role the thermohaline circulation plays in the ocean energy cycle, the meridional heat transport in global ocean is analysed to evaluate the oceanic response to desertification on latitudinal basis. The feedbacks from the mean meridional oceanic heat transport are mapped in Figure 5 for all desertification scenarios. The overall effect of desertification is an increase in annual mean meridional oceanic heat transport. There is a most obvious increase in annual mean meridional oceanic heat transport in most parts of the world as for the simulation Dall because of its associated most pronounced cooling which affects the density of the sea surface water through the atmosphere long-wave radiation. The increase in annual mean meridional oceanic heat transport is largest over the equatorial region and diminishes poleward. The second largest increase in annual mean meridional oceanic heat transport is for D4560 and D1530. This is accounted for the prominent and extensive global cooling (Figure 2) and drying (Figure 4). As for D1530, a smaller increase in oceanic heat transport exists than that in D3045 over low latitudes of the NH. There is a minimum increase in D0015 because of its smaller cooling and drying globally. In fact, this increase in oceanic heat transport can be explained by the cool and dry air in the troposphere. They transmit less long-wave radiation from the atmosphere to the ocean surface. Consequently, less energy is absorbed at the ocean surface, thus leading to a decrease in SSTs (Davin and Noblet-Ducoudré, 2010). This decreased SSTs cause a higher density of the surface water which finally causes increased thermohaline overturning and oceanic heat transport. Such increased heat transport leads to a warming in high latitudes and a retreat of sea ice. The retreat of sea ice leads to a further warming because of the ice-albedo feedback and the increase of the heat supply from the ocean.

4. Discussion

The climatic impact of desertification in the MPM-2 experiment shows a decreased global annual mean surface air

temperature in the range of 0.04–1.76 °C on the basis of latitude bands. A prominent decrease in surface temperature, an increase in land surface albedo and a decrease in precipitation are obtained in the NH in response to vegetation removal in this paper. Also, a maximum local cooling during MAM and JJA are found, as well as an increase in oceanic heat transport.

A global cooling of 0.04–1.76 °C is obtained using the MPM-2 because of replacement of realistic land cover representation by desert on latitude bands basis in the frame of the present study, which is in well agreement with the global cooling revealed by previous simulations because of desertification or vegetation removal. Charney *et al.* (1975) find a radiative heat loss caused by the high albedo of a desert which contributes significantly to the sinking and drying of the air aloft and therefore to the reduction of precipitation. Davin *et al.* (2007) show that forest replacement commonly decreases radiative forcing via an increase in albedo which tends to cool the global climate via the radiation balance. Brovkin *et al.* (2004) demonstrate that biogeophysical mechanisms because of forest removal tend to decrease global air temperature by 0.26 °C. The spread between the results in this study and previous estimates is likely caused by their different model parameterizations and configurations of forest removal. However, the cooling found in this article in response to forest removal is in contradiction with some results. A net global land temperature change of −1.2 °C is obtained by Kleidon *et al.* (2000) with a change from a desert world to a green planet which is because of increased evapotranspiration under the tree scenario. Using a General Circulation Model with fixed SSTs, their simulation influences feedbacks between the land and ocean; any change in land temperature is limited by the effects of the infinite heat reservoir of the ocean. The simulation in this study, by contrast, has been conducted with all the important components (atmosphere, land, ocean, ice sheet and terrestrial biosphere) interacting with each other, which promotes the direct effect of desertification.

A prominent decrease in surface temperature, an increase in land surface albedo as a forcing and a decrease in precipitation as a response are simulated in the NH in
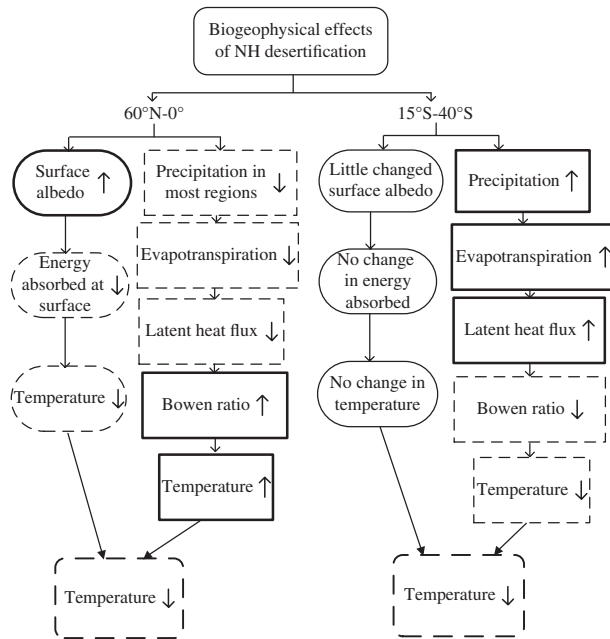
Figure 6. Schematic diagram of NH desertification feedback. Full thick lines indicate increased changes, while dash ones indicate decreased changes. Rectangles indicate surface albedo change as a forcing and ovals indicate precipitation change as a response.

response to vegetation removal in this article (Figure 6), which is consistent with previous studies where the land surface albedo change is the dominating force (Sud *et al.*, 1996; Costa and Foley, 2000). This decrease in surface temperature is accounted for the albedo-change cooling effect which dominates over the evapotranspiration warming effect in response to desertification. The impact of the increased land surface albedo on surface temperature is partly offset by decreased evaporation. Land surface albedo change gives the dominant influence in middle and high latitudes of NH with desert expansion producing net cooling, which is in line with some previous studies. Betts (2001) finds that the global surface temperature change owing to vegetation changes is mainly because of the land surface albedo changes. Betts (2000) and Govindasamy *et al.* (2001) note that forest removal in northern temperate and boreal regions leads to an increase in land surface albedo and consequent cooling. This local cooling is affected by the sea-ice albedo feedback. However, the tropical cooling effects found in this work in response to desertification contradicts results of some AGCM simulations, which shows a net warming effect caused by evapotranspiration (Henderson-Sellers *et al.*, 1993; Costa and Foley, 2000; De Fries *et al.*, 2002). Betts *et al.* (2007) even illustrate that reforestation (or avoided forest removal) in tropical regions could exert a double cooling effect through carbon sequestration and increased evaporation and cloud cover. The spread can be that most of the simulations are performed using AGCMs with prescribed SSTs, which alters the global response considerably. Prescribed SSTs neglect the water vapour response from the sea surface and probably invert the sign of zonally averaged temperature changes (Ganopolski *et al.*, 2001).

Desertification generally causes a lower surface albedo, which can therefore lead to increased shortwave reflection, thus a cooling influence (Douville and Royer, 1997). Also, conversion of forest, cropland or pasture to desert reduces the aerodynamic roughness of the landscape and decreases both the capture of precipitation on the canopy and the root extraction of soil moisture; these changes tend to decrease evaporation and hence reduce the fluxes of moisture and latent heat from the surface to the atmosphere, which acts to increase the temperature near the surface (Lean and Rowntree, 1997; Betts *et al.*, 2007). In the frame of the present study the forest and grass removal in $0°-15°N$ causes a maximum local cooling of $0.38\,°C$ during MAM. While the desert expansions in $15°-30°N$, $30°-45°N$ and $45°-60°N$ cause a most pronounced local cooling of $2.5\,°C$, $1.1\,°C$, $2.2\,°C$ during JJA, respectively. The latitudinal-band desertification has prominent regional effects which are in line with some previous simulations. The larger local changes coincide with large-scale agricultural areas which are showed by Feddema *et al.* (2005). In addition, the prominent cooling during MAM in response to desert expansions over $0°-15°N$ and the maximum JJA cooling owing to desert expansions over $30°-45°N$ are resulted from the cooling effects of land surface albedo which compensate for the warming effects of precipitation decrease. While the desert expansions in $15°-30°N$ and $45°-60°N$ lead to prominent summer coolings over forcing originating areas which are caused by the joint cooling effects of increases in land surface albedo and precipitation.

The simulated cooling of $0.02-0.2\,°C$ in low latitudes of the SH is because of the evapotranspiration cooling effect in response to desertification although the temperature and precipitation trends are not statistically significant in the present simulation. The desert expansion in the NH leads to an increase in precipitation and a rarely change in land surface albedo over low latitudes of the SH (Figure 6). Such increase in precipitation of the SH is a combined result of the NH desertification and associated changes in atmospheric and oceanic meridional transport of energy. This precipitation increase provides more water availability to evapotranspiration thus producing cooling effect in low latitudes of the SH. This less-prominent feedback from SH is in line with earlier studies. Brovkin *et al.* (2006) show that a less-significant response in the SH is accounted for the geographical distribution of the forcing and the much smaller land masses in the SH.

The desertification in the NH leads to an increase in oceanic heat transport in this paper. Decreased SSTs associated with cooling surface air in response to forest and grass replacement cause a higher density of the surface water which leads to increased thermohaline overturning and oceanic heat transport. This is in consistent with some previous studies. Brovkin *et al.* (2003) and Rahmstorf *et al.* (1996) demonstrate that increased SSTs result in lower density of the surface water, thus decreasing thermohaline overturning and northward oceanic heat transport.

These results also suggest that teleconnection patterns because of desert expansion which have already occurred are capable of affecting the temperature, precipitation and oceanic heat transport distributions worldwide and may have already done so. Such teleconnection pattern is in line with some previous studies. Souza (2006) finds that total desertification of SANEB area would affect local and regional climate. This teleconnected effects are traditionally unaccounted for in global climate trend analyses (North and Stevens, 1998) but growing evidence indicates that these effects should be emphasized in desertification research (Verstraete *et al.*, 2008), which necessitates further examination of their scope and significance (Chase *et al.*, 2000; Findell *et al.*, 2009).

It should be noted that the MPM-2 used in this study has several limitations. Because of many simplifications of the physical and dynamical processes and the low-model resolution, it does not include certain details, such as detailed atmospheric circulations and cloud dynamics. So there are still some limitations about rainfall in our simulations. As for cloud feedback which affects the climate response, some models simulate a decrease in cloud cover which leads to increased global shortwave radiation absorption in response to surface cooling. The effect of such decreased cloud cover would counteract the effect of increased surface albedo on net radiative fluxes because of forest and grass removal. Because of the absence of the cloud feedback, the climate response is probably to be dampened in the simulation. Also, the desertification experiment designed here is an extreme case, which is probably not realistic. In further analysis of desertification effects on climate, the challenge will be to find the key land parameters and their relative significance as well as the detailed interactions of these parameter changes in response to desertification.

5. Conclusion

The future of a billion people in dry-lands whose livelihoods depend on natural resources is at risk from desertification exacerbated by climate change. Research into the effects of desertification on climate contributes to humans' adaptation to desertification. Our study demonstrates that desertification affects climate locally and globally in the present simulation. There is a significant model sensitivity to five scenarios of desertification, with a biogeophysical cooling range of 0.04–1.76 °C among the simulations at the global scale. The desertification leads to different cooling effects on climate over forcing originating areas. The desert expansions in 15°–30°N and 45°–60°N cause most prominent coolings of 2.5 and 2.2 °C during JJA. Furthermore, the desertification leads to an increase in annual mean meridional oceanic heat transport with a maximum increase in desert expansion of 45°–60°N over most areas. These results indicate that desertification in 15°–30°N and 45°–60°N produces a more prominent effect on the Earth's climate and even oceanic circulation which should be paid more attention to.

References

Alkama R, Kageyama M, Ramstein G. 2012. A sensitivity study to global desertification in cold and warm climates: results from the IPSL OAGCM model. *Clim. Dyn.* **38**: 1629–1647.

Anderson-Teixeira KJ, Snyder PK, Twine TE, Cuadra SV, Costa MH, DeLucia EH. 2012. Climate-regulation services of natural and agricultural ecoregions of the Americas. *Nat. Clim. Change* **2**: 177–181.

Ash AJ, Stafford Smith DM, Abel N. 2002. Land degradation and secondary production in semi-arid and arid grazing systems: what is the evidence?. In *Global Desertification: Do Humans Cause Deserts?*, Reynolds JF, Stafford Smith DM (eds). Dahlem University Press: Berlin, 111–134.

Asner GP, Heidebrecht KB. 2005. Desertification alters regional ecosystem–climate interactions. *Glob. Change Biol.* **11**: 182–194.

Bala G, Caldeira K, Wickett M, Phillips TJ, Lobell DB, Delire C, Mirin A. 2007. Combined climate and carbon-cycle effects of large-scale deforestation. *Proc. Natl. Acad. Sci. U.S.A.* **104**: 6550–6555.

Betts RA. 2000. Offset of the potential carbon sink from boreal forestation by decreases in surface albedo. *Nature* **408**: 187–200.

Betts RA. 2001. Biogeophysical impacts of land use on present day climate: near-surface temperature and radiative forcing. *Atmos. Sci. Lett.* **2**: 39–51.

Betts RA, Falloon PD, Goldewijk KK, Ramankutty N. 2007. Biogeophysical effects of land use on climate: model simulations of radiative forcing and large-scale temperature change. *Agric. For. Meteorol.* **142**: 216–233.

Bonan GB. 1997. Effects of land use on the climate of the United States. *Clim. Change* **37**: 449–486.

Bonan GB. 2008. Forests and climate change: forcings, feedbacks, and the climate benefits of forests. *Science* **320**: 1444–1449.

Bonan GB, Pollard D, Thompson SL. 1992. Effects of boreal forest vegetation on global climate. *Nature* **359**: 716–718.

Bounoua L, DeFries R, Collatz GJ, Sellers P, Khan H. 2002. Effects of land cover conversion on surface climate. *Clim. Change* **52**: 29–64.

Brovkin V, Ganopolski A, Svirezhev Y. 1997. A continuous climate-vegetation classification for use in climate-biosphere studies. *Ecol. Model.* **101**: 251–261.

Brovkin V, Ganopolski A, Claussen M, Kubatzki C, Petoukhov V. 1999. Modelling climate response to historical land cover change. *Glob. Ecol. Biogeogr.* **8**: 509–517.

Brovkin V, Levis S, Loutre M, Crucifix M, Claussen M, Ganopolski A, Kubatzki C, Petoukhov V. 2003. Stability analysis of the climate-vegetation system in the northern high latitudes. *Clim. Change* **57**: 119–138.

Brovkin V, Sitch S, Von Bloh W, Claussen M, Bauer E, Cramer W. 2004. Role of land cover changes for atmospheric CO$_2$ increase and climate change during the last 150 years. *Glob. Change Biol.* **10**: 1253–1266.

Brovkin V, Claussen M, Driesschaert E, Fichefet T, Kicklighter D, Loutre MF, Matthews HD, Ramankutty N, Schaeffer M, Sokolov A. 2006. Biogeophysical effects of historical land cover changes simulated by six Earth system models of intermediate complexity. *Clim. Dyn.* **26**: 587–600.

Brovkin V, Raddatz T, Reick CH, Claussen M, Gayler V. 2009. Global biogeophysical interactions between forest and climate. *Geophys. Res. Lett.* **36**: L07405, doi: 10.1029/2009GL037543.

Charney JG, Stone PH, Quirk WJ. 1975. Drought in the Sahara: a biogeophysical feedback mechanism. *Science* **187**: 434–435.

Chase TN, Pielke RA, Kittel TGF, Nemani RR, Running SW. 2000. Simulated impacts of historical land cover changes on global climate in northern winter. *Clim. Dyn.* **16**: 93–105.

Claussen M, Brovkin V, Ganopolski A. 2001. Biogeophysical versus biogeochemical feedbacks of large-scale land cover change. *Geophys. Res. Lett.* **28**: 1011–1014.

Costa MH, Foley J. 2000. Combined effects of deforestation and doubled atmosphere CO_2 concentration on the climate of Amazonia. *J. Clim.* **13**: 18–24.

Davin EL, Noblet-Ducoudré ND. 2010. Climatic impact of global-scale deforestation: radiative versus nonradiative processes. *J. Clim.* **23**: 97–112.

Davin EL, Noblet-Ducoudre ND, Friedlingstein P. 2007. Impact of land cover change on surface climate: relevance of the radiative forcing concept. *Geophys. Res. Lett.* **34**: L13702, doi: 10.1029/2007GL029678.

De Fries RS, Bounoua L, Collatz GJ. 2002. Human modification of the landscape and surface climate in the next fifty years. *Glob. Change Biol.* **8**: 438–458.

Douville H, Royer JF. 1997. Influence of the temperate and boreal forests on the Northern Hemisphere climate in the Meteo-France climate model. *Clim. Dyn.* **13**: 57–74.

Feddema J, Oleson K, Bonan G, Mearns L, Washington W, Meehl G, Nychka D. 2005. A comparison of a GCM response to historical anthropogenic land cover change and model sensitivity to uncertainty in present-day land cover representations. *Clim. Dyn.* **25**: 581–609.

Findell KL, Shevliakova E, Milly PCD, Stouffer RJ. 2007. Modeled impact of anthropogenic land cover change on climate. *J. Clim.* **20**: 3621–3634.

Findell KL, Pitman AJ, England MH, Pegion PJ. 2009. Regional and global impacts of land cover change and sea surface. *J. Clim.* **22**: 3248–3269.

Forest CE, Stone PH, Sokolov AP. 2002. Quantifying uncertainties in climate system properties with the use of recent climate observations. *Science* **295**: 113–117.

Ganopolski A, Petoukhov V, Rahmstorf S, Brovkin V, Claussen M, Eliseev A, Kubatzki C. 2001. CLIMBER-2: a climate system model of intermediate complexity. Part II: model sensitivity. *Clim. Dyn.* **17**: 735–751.

Giannini A, Biasutti M, Verstraete MM. 2008. A climate model-based review of drought in the Sahel: desertification, the re-greening and climate change. *Glob. Planet. Change* **64**: 119–128.

Govindasamy B, Duffy PB, Caldeira K. 2001. Land use changes and Northern Hemisphere cooling. *Geophys. Res. Lett.* **28**(2): 291–294.

Henderson-Sellers A, Dickinson RE, Durbidge TB, Kennedy PJ, Mcguffie K, Pitman AJ. 1993. Tropical deforestation – modeling local-scale to regional-scale climate change. *J. Geophys. Res.* **98**: 7289–7315.

Hill J, Megier J, Mehl W. 1995. Land degradation, soil erosion and desertification monitoring in Mediterranean ecosystems. *Remote Sens. Rev.* **12**: 107–130.

IPCC. 2013. Climate Change 2013: The Physical Science Basis. Contribution of WGI to the Fifth Assessment Report of IPCC, Stocker TF, Qin D, Plattner G-K, Tignor M, Allen SK, Boschung J, Nauels A, Xia Y, Bex V, Midgley PM (eds). Cambridge University Press, Cambridge, UK and New York, NY.

Kleidon A, Fraedrich K, Heimann M. 2000. A green planet versus a desert world: estimating the maximum effect of vegetation on the land surface climate. *Clim. Change* **44**: 471–493.

Lean J, Rowntree PR. 1997. Understanding the sensitivity of a GCM simulation of Amazonian deforestation to the specification of vegetation and soil characteristics. *J. Clim.* **10**: 1216–1235.

Lee X, Goulden ML, Hollinger DY, Barr A, Black TA, Bohrer G, Bracho R, Drake B, Goldstein A, Gu L, Katul G, Kolb T, Law BE, Margolis H, Meyers T, Monson R, Munger W, Oren R, Paw UKT, Richardson AD, Schmid HP, Staebler R, Wofsy S, Zhao L. 2011. Observed increase in local cooling effect of deforestation at higher latitudes. *Nature* **479**: 384–387.

Li SG, Harazono Y, Oikawa T, Zhao HL, He ZY, Chang XL. 2000. Grassland desertification by grazing and the resulting micrometeorological changes in Inner Mongolia. *Agric. For. Meteorol.* **102**: 125–137.

Marshall SJ, Clarke GKC. 1997. A continuum mixture model of ice stream thermomechanics in the Laurentide Ice Sheet, 1. Theory. *J. Geophys. Res.* **102**: 20599–20613.

North GR, Stevens MJ. 1998. Detecting climate signals in the surface temperature record. *J. Clim.* **11**: 563–577.

Pielke RA, Marland G, Betts RA, Chase TN, Eastman JL, Niles JO, Niyogi DDS, Running SW. 2002. The influence of land-use change and landscape dynamics on the climate system: relevance to climate-change policy beyond the radiative effect of greenhouse gases. *Philos. Trans. R. Soc. Lond. A* **360**: 1705–1719.

Pitman AJ, Noblet-Ducoudré ND, Cruz FT, Davin EL, Bonan GB, Brovkin V, Claussen M, Delire C, Ganzeveld L, Gayler V, van den Hurk BJJM, Lawrence PJ, van der Molen MK, Muller C, Reick CH, Seneviratne SI, Strengers BJ, Voldoire A. 2009. Uncertainties in climate responses to past land cover change: first results from the LUCID intercomparison study. *Geophys. Res. Lett.* **36**: L14814, doi: 10.1029/2009GL039076.

Pongratz J, Reick C, Raddatz T, Claussen M. 2008. A reconstruction of global agricultural areas and land cover for the last millennium. *Glob. Biogeochem. Cycles* **22**: GB3018, doi: 10.1029/2007GB003153.

Rahmstorf S, Marotzke J, Willebrand J. 1996. Stability of the thermohaline circulation. In *The Warm Water Sphere of the North Atlantic Ocean*, Krauss W (ed). Borntraeger: Stuttgart, Germany, 129–158.

Reynolds JF, Stafford Smith DM. 2002. *Global Desertification: Do Humans Cause Deserts?*, Vol. 88. Dahlem University Press: Berlin.

Shi Z, Yan X, Yin C, Wang Z. 2007. Effects of historical land cover changes on climate. *Chin. Sci. Bull.* **18**: 2575–2583.

Souza SS. 2006. *Regional climatic impacts of the vegetation change in the semi-arid in Northeast Brazil*. PhD dissertation (in Portuguese). Dissertation, Instituto Nacional de Pesquisas Espaciais. http://www.inpe.br/biblioteca (accessed 30 April 2010).

Souza DC, Oyama MD. 2011. Climatic consequences of gradual desertification in the semi-arid area of Northeast Brazil. *Theor. Appl. Climatol.* **103**: 345–357.

Sud YC, Walker GK, Kim JH, Liston GE, Sellers PJ, Lau WKM. 1996. Biogeophysical consequences of a tropical deforestation scenario: a GCM simulation study. *J. Clim.* **9**: 3225–3247.

United Nations Sudano Sahelian Office. 2002. *Drylands: An Overview*. UNDP/DDC, Nairobi.

Verstraete MM, Brink AB, Scholes RJ, Beniston M, Smith MS. 2008. Climate change and desertification: where do we stand, where should we go? *Glob. Planet. Change* **64**: 105–110.

Wang G, Eltahir EAB. 2000. Ecosystem dynamics and the Sahel drought. *Geophys. Res. Lett.* **27**(6): 795–798.

Wang Z, Mysak LA. 2000. A simple coupled atmosphere–ocean–sea ice-land surface model for climate and paleoclimate studies. *J. Clim.* **13**: 1150–1172.

Wang Z, Mysak LA. 2001. Ice sheet-thermohaline circulation interactions in a climate model of intermediate complexity. *J. Oceanogr.* **57**: 481–494.

Wang Z, Mysak LA. 2002. Simulation of the last glacial inception with the green McGill Paleoclimate Model. *Geophys. Res. Lett.* **32**: L12705, doi: 10.1029/2005GL023047.

Wang Y, Yan X. 2013. Climate responses to historical land cover changes. *Clim. Res.* **56**: 147–155.

Wang Z, Mysak LA, McManus JF. 2002. Response of the thermohaline circulation to cold climates. *Paleoceanography* **17**(1): 1006, doi: 10.1029/2000PA00587.

Wang Y, Mysak LA, Wang Z, Brovkin V. 2005a. The greening of the McGill Paleoclimate Model. Part II: simulation of Holocene millennial-scale natural climate changes. *Clim. Dyn.* **24**: 481–496.

Wang Y, Mysak LA, Roulet NT. 2005b. Holocene climate and carbon cycle dynamics: experiments with the "green" McGill Paleoclimate Model. *Glob. Biogeochem. Cycles* **19**: GB3022, doi: 10.1029/2005GB002484.

Wang Y, Mysak LA, Wang Z, Brovkin V. 2005c. The greening of the McGill paleoclimate Model. Part I: improved land surface scheme with vegetation dynamics. *Clim. Dyn.* **24**: 469–480.

Wang Y, Yan X, Wang Z. 2013. Simulation of the influence of historical land cover changes on the global climate. *Ann. Geophys.* **31**: 995–1004.

Warren A, Khogali M. 1992. *An Assessment of Desertification and Drought in the Sudano-Sahelian Region*. United Nations Sudano-Sahelian Office: New York, NY.

Williams MAJ, Balling RC. 1994. *Interactions of Desertification and Climate*. WMO and UNEP: Geneva, Switzerland and Nairobi.

Yin CH, Yan XD, Shi ZG, Wang ZM. 2007. Simulation of the climatic effects of natural forcings during the pre-industrial era. *Chin. Sci. Bull.* **11**: 1545–1558.

Zeng N, Neelin JD, Lau K-M, Tucker CJ. 1999. Enhancement of interdecadal climate variability in the Sahel by vegetation interaction. *Science* **286**: 1537–1540.

Zheng X, Eltahir EAB. 1997. The response to deforestation and desertification in a model of West African monsoons. *Geophys. Res. Lett.* **24**(2): 155–158.

Zwiers FW, von Storch H. 1995. Taking serial correlation into account in tests of the mean. *J. Clim.* **8**: 336–351.